ORIGINAL ARTICLE

SU2 Conference 2020, June 10-12, 2020

Numerical Simulation of Flow over NACA-0012 Airfoil Pitching at Low Frequencies

Aasha GC[1] | Vishal Raj[1] | Ramesh Kolluru[2] | Ramesh M. Chalkapure[1] | Rohan Srikanth[1] | Ajit H.A.[1]

[1]Department of Mechanical Engineering, BMS College of Engineering, Bengaluru, Karnataka, 560019, India

[2]PDF, Department of Aerospace Engineering, Indian Institute of Science, Bengaluru, Karnataka, 560012, India

Correspondence
Aasha GC, Department of Mechanical Engineering, BMS College of Engineering, Bengaluru, Karnataka, 560019, India
Email: aashagc0@gmail.com

Oscillating structures find numerous applications in aerospace and automobile industries. The flow over these structures primarily depends on the frequency of oscillation and the speed of the incoming flow. If the pitching frequency of the airfoil is low, the flow can be idealized as a quasi-steady flow at various angles of attack. In the present work, an attempt is made to numerically simulate the flow over the symmetrical airfoil NACA-0012, pitching at low frequencies, using the open-source CFD-code SU2. The airfoil is pitched at an angular frequency of $0.15707 \frac{rad}{sec}$, over an amplitude of 9° about a mean angle of 0°. The dynamic flow behavior and aerodynamic characteristics are compared with the static simulations carried out within the same range of angles of attack.

KEYWORDS
pitching, *static*, *NACA-0012*, *angular frequency*, *quasi-steady*

1 | INTRODUCTION

On geological time-scales, man has mastered aerial and underwater locomotion only very recently, while the animals ruling the sky and the seas evolved the necessary, and often fascinating, means of locomotion long before the earliest

Abbreviations: CFD, Computational Fluid Dynamics; AoA, angle of attack in degrees

human ancestors. The complexity and ruthless efficiency of these marvels of evolution have fascinated mankind and fuelled man's own desire to master the endless sky and the mystic seas. The long-range flight in birds, insects and bats, known as powered flight, actively involves muscle movements to generate the flapping motion of wings. Many species of aquatic animals have evolved hydrofoil-like fins and flippers, which they beat in a periodic motion to generate lift. Another commonly observed means of propulsion is through an undulating movement of the entire body, or parts of it, in a wave-like motion, thus generating the thrust to propel them in water. A deeper understanding of such flapping-wing and undulating-body aerodynamics and hydrodynamics can help build more efficient aerial and underwater vehicles. Hence, the need to investigate into, understand and replicate the biomechanics of locomotion of animals in air and water, that employ pitching motion of one or more body parts, becomes imperative. Fortunately, using modern CFD techniques, it is possible to theoretically replicate the flow physics and biomechanics of such locomotion to an appreciable extent. Moreover, pitching motion of airfoils has already been put to use by man in both aerial domain, like ailerons, flaps and elevators in aircraft, and underwater regimes, as in parts of submarines, Autonomous Underwater Vehicles (AUVs) and Remotely Operated Vehicles (ROVs).

An airfoil pitching sinusoidally results in a periodic yet unsteady flow, as it is characterized by a time-dependent evolution of the physical quantities and aerodynamic coefficients. One of the factors that significantly influences the temporal variation of aerodynamic coefficients and flow parameters is the so-called *reduced frequency*, k. It is a non-dimensional expression of the angular frequency at which the pitching occurs, given by the expression $k = (\omega \times b)/v$, where, ω is the angular frequency, b is the semi-chord length and v is the flow velocity. If the reduced frequency is high, the aerodynamic response of the body suffers a significant phase lag with respect to the temporal variations in flow conditions [1]. However, if the reduced frequency is very low, the phase lag is negligible and the aerodynamic response of the body remains in sync with its pitching motion. Hence, the resulting flow behavior around a slowly pitching airfoil at a particular angle is expected to be similar to that for a static airfoil at the same angle. This type of flow is known as a quasi-steady flow, in which the temporal changes in the mean-flow properties are so slow that the flow could rather be treated as steady. The following study intends to shed greater light on this specific regime of unsteady flows, namely quasi-steady flow. Previous studies done on a wide range of reduced frequencies at different Reynolds numbers (Re) have demonstrated, both numerically and experimentally, that the reduced frequency has a significant effect on the resulting flow behavior, as well as the nature of dynamic vortices for larger angles. Numerical analyses done by Zhang et al. [2], Yu et al. [3] and Kurtulus et al. [4] discuss the pronounced effects of reduced frequency on the resulting flow pattern and vortex generation on an oscillating airfoil pitching sinusoidally at different reduced frequencies and Reynolds numbers. Pechloff et al. [5] have presented a numerical analysis on a pitching airfoil, done using the noncommercial CFD-code FLOWer, for a very similar value of Reynolds number and time step size as the current study. Another interesting study is the numerical investigation of vortex behavior and flow structure during dynamic stall of an oscillating pitching hydrofoil done by Karbasian et al. [6]. Experimental examinations of flow behavior around a pitching airfoil have been carried out by Lee et al. [7] and Sharma et al. [8].

The main objective of the current study is to numerically analyze the nature of flow and the flow coefficients around a slowly pitching airfoil using SU2. The flow is incompressible, with a velocity of $30 ms^{-1}$ and at $Re = 2.9 \times 10^5$. The sinusoidal pitching motion used is described by equation (1).

$$\alpha(t) = \alpha_0 + \alpha_a sin\omega t \tag{1}$$

where, α is the angle of attack in degrees that varies with time, α_o is the mean angle of attack, α_a is the amplitude, ω is the frequency in radians per second, and t is the time in seconds. A mean angle of 0°, an amplitude of 9° and an angular frequency of $0.15707 \frac{rad}{sec}$ are chosen in order to maintain quasi-steady conditions.

2 | NUMERICAL METHODOLOGY

2.1 | Governing Equations

The governing equations used are incompressible Navier-Stokes equations, [9], as given in Eqn (2).

$$R(v) = \partial_t V + \nabla.\overline{F}^c(V) - \nabla.\overline{F}^v(V, \nabla V) - S = 0 \tag{2}$$

where,

$$V = \begin{pmatrix} p \\ \bar{v} \\ T \end{pmatrix}, \ \overline{F}^c(V) = \begin{pmatrix} \rho\bar{v} \\ \rho\bar{v} \otimes \bar{v} + \bar{\bar{I}}p \\ \rho c_p T \bar{v} \end{pmatrix}, \ \overline{F}^v(V) = \begin{pmatrix} \cdot \\ \bar{\bar{\tau}} \\ \kappa\nabla T \end{pmatrix}, \ \overline{v} = \begin{pmatrix} u \\ v \\ w \end{pmatrix}$$

In the above equations, the computational vector V refers to the vector of working variables within the solver, which are pressure p, velocity vector $\overline{v}$ and temperature T for the mass, momentum and energy equations, respectively. The vector of convective fluxes $\overline{F}^c$ indicates the convective transport of physical quantities, namely mass, momentum and energy, in the fluid. Variables ρ and c_p are the fluid density and specific heat at constant pressure respectively. It also includes the isotropic pressure component $\bar{\bar{I}}$ in the momentum equation. The vector of viscous fluxes $\overline{F}^v$ comprises of the viscous stresses $\bar{\bar{\tau}} = \mu(\nabla\overline{v} + \nabla\overline{v}^T) - \mu\frac{2}{3}\bar{\bar{I}}(\nabla \cdot \overline{v})$, and heat diffusion due to molecular thermal conduction $\kappa\nabla T$. The viscosity coefficient μ and thermal conductivity coefficient κ need to be further determined to close the equations. The last of all the terms is the source term S, which contains all the volume sources due to body forces and volumetric heating.

Chorin's method of artificial compressibility [10] employed in SU2 is used to attain pressure-velocity coupling. Incompressible Reynolds-Averaged Navier-Stokes (INC_RANS) equations with the $k-\omega$ SST turbulence model are used for solving the incompressible form of the governing equations. For the purpose of spatial discretization, SU2 uses the cell-vertex scheme with median-dual control volumes. Flux-difference splitting (FDS) and Green-Gauss schemes are used in the current study as the flow convective and gradient methods, respectively [11]. Whereas, Implicit Euler method is used as the time discretization method.

The time derivative here does not represent a true physical time, it is rather a fictitious time known as *pseudo-time*. This modified set of Navier-Stokes equations are then solved at each time-level using the iterative solver Flexible Generalized Minimal Residual (FGMRES), so as to attain a steady-state at each of those time-levels.

2.2 | Parameters Used in Simulations

The numerical values as well as the numerical methods applied for carrying out the simulations are tabulated in Table 1 and Table 2.

2.3 | Grid and Boundary Conditions

A C-type grid is used around the airfoil with Farfield boundary placed at a distance of 500c. SU2_DEF feature available in SU2 is used to resize the original grid with a unit chord length (c) to a chord length of 0.15 m. Three grids of different fineness, as shown in Table 3, are used in the study to ensure grid independence. These grids, among many others,

TABLE 1 Flow Parameters and Their Values

Flow Parameter	Value	Flow Parameter	Value
Velocity	30 ms^{-1}	Reynolds number	2.9×10^5
Chord length	0.15 m	Reduced frequency	0.0004
Temperature	298 K	Mean pitching angle	0°
Density	$1.2kgm^{-3}$	Pitching amplitude	9°
Dynamic viscosity	$1.8e-5kgm^{-1}s^{-1}$	Pitching axis	$0.25c$

TABLE 2 Numerical Parameters and Their Values/Methods

Numerical Parameter	Value/Method	Numerical Parameter	Value/Method
Solver	Incompressible RANS	Time marching	Dual Time Stepping - 2nd Order
Turbulence model	SST	Slope limiter	Venkatkrishnan
Reference length	0.15	Multigrid level	0
Time step	$0.11111s$	Time discretization	Euler Implicit Scheme
Maximum time	$200s$	Gradient method	Green Gauss Scheme
Surface movement	Deforming	Flow convective method	Flux Difference Splitting (FDS)
Density model	Constant	Turbulent conv. method	Scalar Upwind
Viscosity model	Constant	MUSCL scheme	Yes
Energy equation	No (Heat Transfer absent)	Convergence criteria	Residual
Preconditioner	LINELET	Limiting residual value	$1e-6$
Linear solver	FGMRES	Output files	flow, surface_flow, solution_flow

are available on [12].

TABLE 3 Grid Nomenclature

Grid Nomenclature	Grid	Overall Points	Points on The Airfoil
COARSE	122×65	14576	0.15
MEDIUM	449×129	57824	256
FINE	897×257	230336	512

Dynamic meshing capabilities of SU2 are used to mimic the pitching motion of the airfoil. One such methodology, Volumetric Deformation, is applied for the current study through the SURFACE_MOVEMENT option. In this method, at each time step, the surface boundary (in this case, the airfoil) is first moved, followed by the deformation of the

volume grid to accommodate the new surface position. Further details regarding the same can be obtained from [13]. The figure 1 shows a grid at 0° AoA and at 9° AoA.

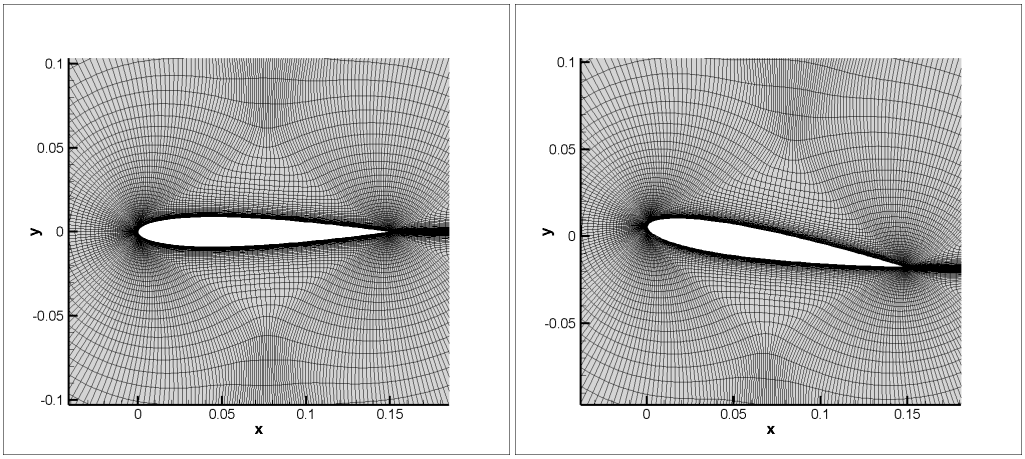

FIGURE 1 Grid at 0° AoA (left) and 9° AoA (right)

The boundary conditions used for the current study are: Farfield Boundary Condition, to represent the free-stream at infinity such that the effect of the finite nature of the domain on the solution is insignificant, and the No-Slip Wall Boundary Condition, to enforce zero relative velocity between the airfoil surface and the viscous fluid.

3 | RESULTS

The following section discusses the results obtained from a pitching airfoil at reduced frequencies. A comparative analysis of results is carried out between static and dynamic cases. The results for the pitching cases have been derived from the fourth pitching cycle, after the initial phase of flow development has been surpassed.

3.1 | Flow Coefficients

3.1.1 | Coefficient of Drag (Cd)

The Coefficient of Drag (Cd) curves for all the grids for both the static and dynamic cases are as shown in Figure 2. The value of Cd increases rapidly as the magnitude of AoA increases, due to increasing resistance offered by the airfoil to the flow. Drag force is minimum for 0° AoA as the airfoil is best aligned with the flow at this angle. It is observed from the patterns of the Cd curves that the profile of Cd doesn't change from medium to fine grids, which effectively shows the solution is grid independent. Also, the similarity of the pitching results with those of static is in accordance with the quasi-steady nature of the flow being studied. Hysteresis effects in the case of pitching results are seen to increase as fineness of the grid increases, and is maximum for the finest grid.

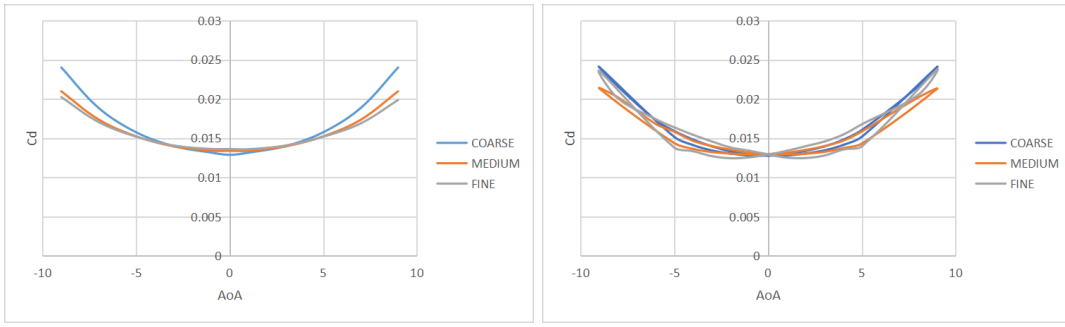

(a) Static Case (b) Dynamic Case

FIGURE 2 Cd vs AoA for COARSE, MEDIUM and FINE Grids

3.1.2 | Coefficient of Lift (Cl)

The values of Coefficient of Lift (Cl), shown in Figure 3a and Figure 3b for the static and pitching cases respectively, are observed to be linear. The airfoil is not seen to stall for any of the three grids in either pitching or static case. Lift force increases in magnitude, as the magnitude of AoA increases, due to the increasing difference in pressure between the upper and lower surfaces. The values of Cl obtained from all three of the grids are in excellent agreement with each other, with hysteresis effects being practically negligible. A comparative analysis of the Cl curves for both the static and pitching cases shows that the values are practically the same. This observed similarity in values is consistent with the characteristics of a quasi-steady flow.

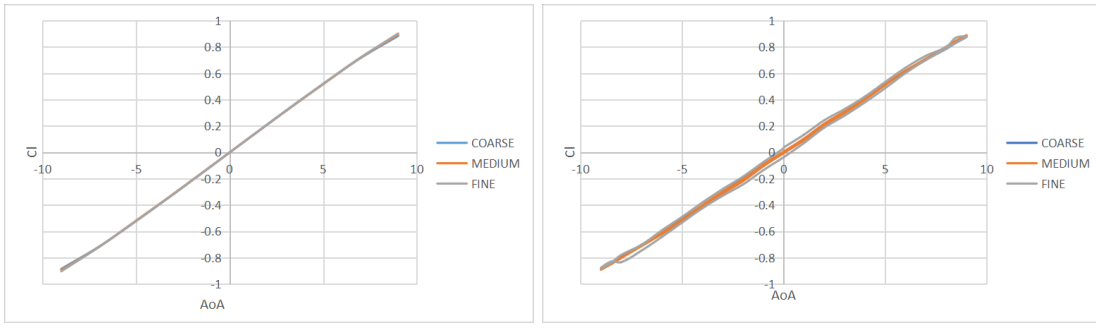

(a) Static Case (b) Dynamic Case

FIGURE 3 Cl vs AoA for COARSE, MEDIUM and FINE Grids

3.1.3 | Coefficient of Moment (Cm)

Figure 4a and Figure 4b show the values of Coefficient of Moment (Cm) for static and pitching cases respectively, about an axis perpendicular to the airfoil. A positive (anticlockwise) moment is generated for negative AoA and a negative (clockwise) moment for positive AoA. The pitching results for the coarse and medium grid bear a good resemblance to the corresponding static results. However, the fine grid is seen to have significant hysteresis effects. The Cm plots also retain the expected nature of a quasi-steady flow.

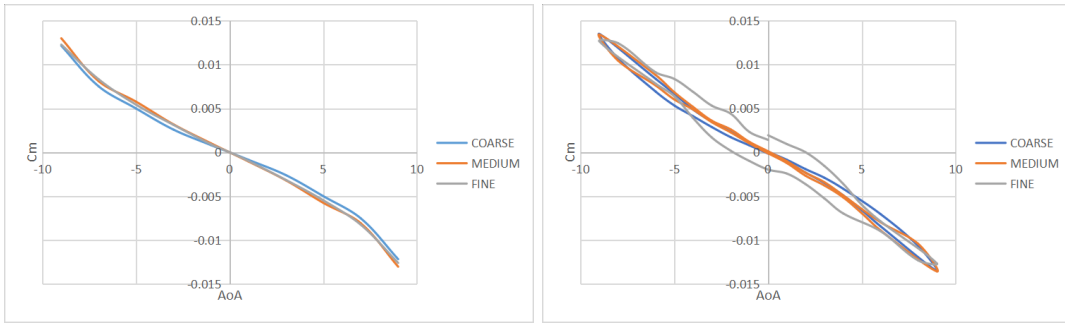

(a) Static Case (b) Dynamic Case

FIGURE 4 Cm vs AoA for COARSE, MEDIUM and FINE Grids

3.1.4 | Pressure Coefficient (Cp)

Figure 5 shows the Pressure Coefficient (Cp) vs x/c (here, x is the x-coordinate distance of the specific point from the leading edge) plots at $-5°, 0°$ and $9°$ AoA for both static and pitching cases. As the angular velocity during pitching is very low, the values of Cp for the pitching cases are virtually the same as those for the static cases, thus demonstrating that the flow behavior in the vicinity of the airfoil is similar for both the cases. The curves for the pitching and static cases are seen to overlap almost perfectly for all the three grids, which signifies that the phase-lag in the response of the airfoil to the slowly changing flow direction is practically non-existent for quasi-steady conditions.

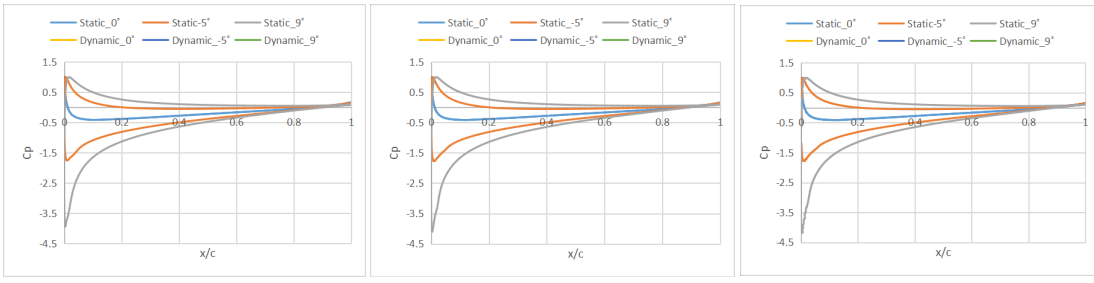

(a) COARSE (b) MEDIUM (c) FINE

FIGURE 5 Cp vs x/c for Static and Dynamic cases

3.2 | Pressure and Velocity Contours

Figure 6, 7, 8 and Figure 9, 10, 11 show the pressure contours and velocity contours respectively at $0°, -5°$ and $9°$ AoA for static and pitching cases. The contours for the pitching case are seen to be quite similar in nature to those for the corresponding static case. No vortex formation or boundary layer turbulence is seen to occur for either static or dynamic case. Flow is smooth and attached throughout the airfoil surface, and there is no occurrence of static or dynamic stall throughout the range of angles studied.

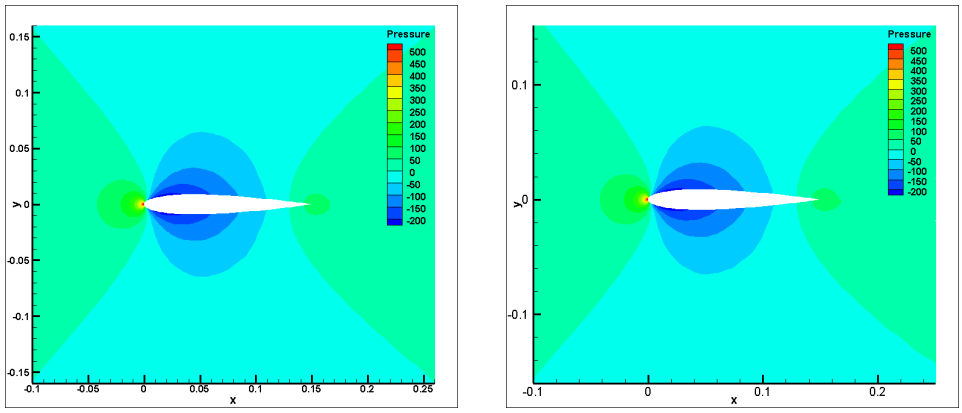

(a) Static Case (b) Dynamic Case

FIGURE 6 Pressure Contours for the COARSE Grid at 0° AoA

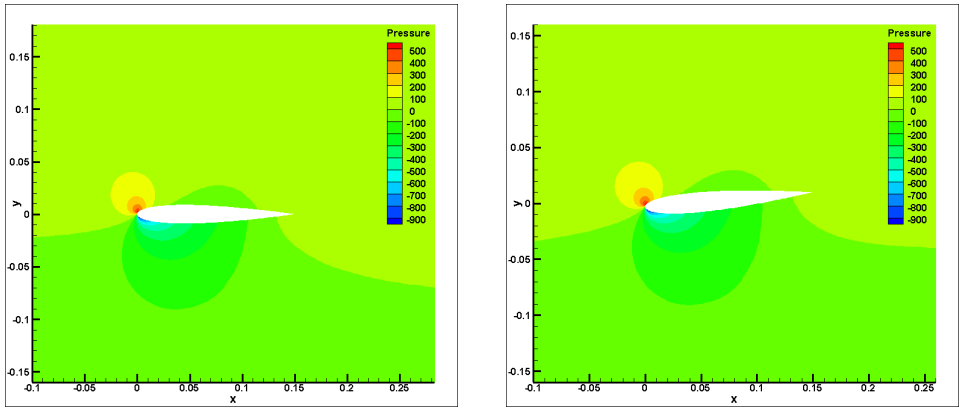

(a) Static Case (b) Dynamic Case

FIGURE 7 Pressure Contours for the MEDIUM Grid at −5° AoA

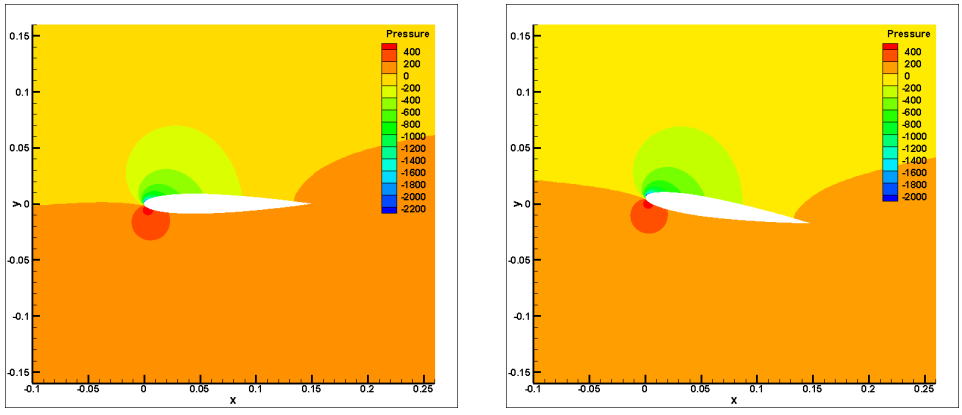

(a) Static Case (b) Dynamic Case

FIGURE 8 Pressure Contours for the FINE Grid at 9° AoA

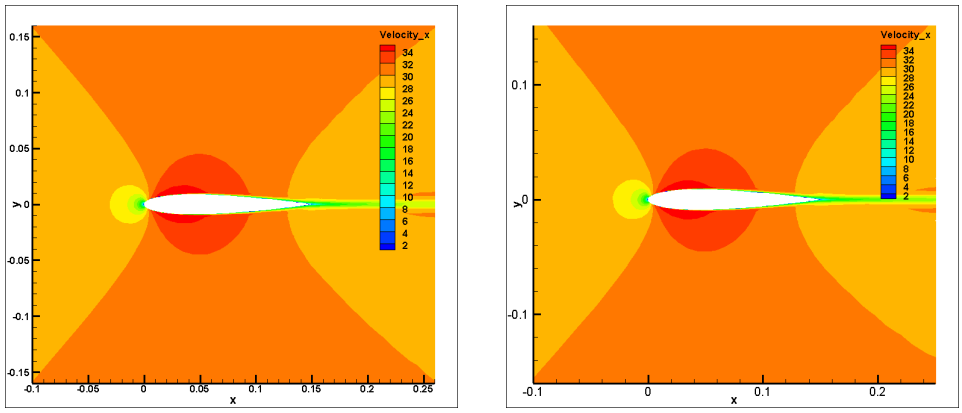

(a) Static Case (b) Dynamic Case

FIGURE 9 Velocity Contours for the COARSE Grid at 0° AoA

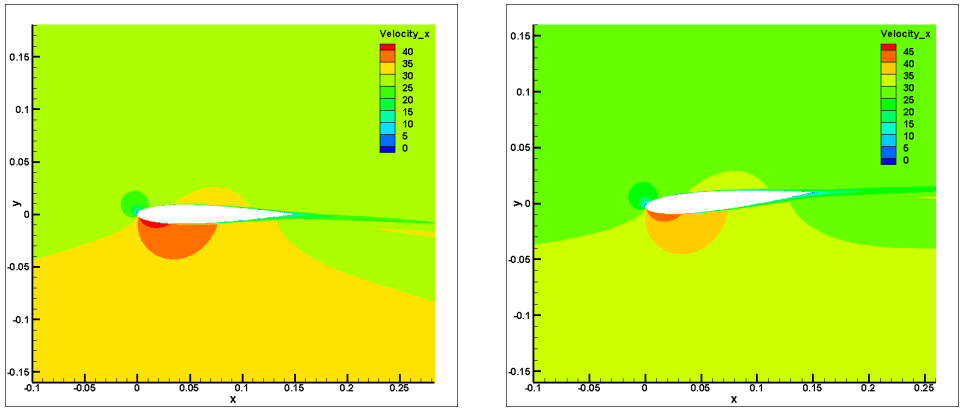

(a) Static Case (b) Dynamic Case

FIGURE 10 Velocity Contours for the MEDIUM Grid at −5° AoA

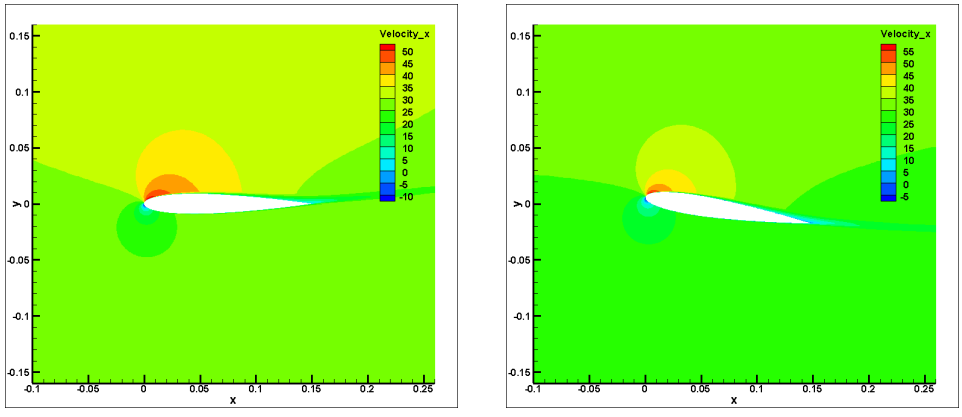

(a) Static Case (b) Dynamic Case

FIGURE 11 Velocity Contours for the FINE Grid at 9° AoA

4 | CONCLUSION

A numerical analysis has been carried out on a slowly pitching symmetrical airfoil NACA-0012 at low reduced frequencies, using dynamic meshing capabilities of open-source CFD-code SU2. The low angular frequency and low Mach number of the flow lead to quasi-steady flow conditions, wherein the results obtained from numerical simulations on the pitching airfoil are expected to closely resemble those from the stationary airfoil at the same angle of attack. Grid independence studies are carried out on three different set of grids and aerodynamic coefficients as well as pressure and velocity contours have been plotted and compared. It is observed that the values of flow parameters obtained from dynamic meshing closely resemble those for the static cases at a given angle of attack. Slow pitching motion of bodies is quite common in nature as well as human engineering applications. The current study has examined the domain of such motion and the results so obtained can be used to further the study of pitching motion of bodies. Moreover, an analysis of the flow behavior under conditions of low reduced frequency can be used as a reference for studies involving relatively faster pitching mechanisms, widening the range of angles studied as well.

references

[1] Abbott IH, Von Doenhoff AE. Theory of wing sections: including a summary of airfoil data. Courier Corporation; 2012.

[2] Zhang M, Wu Q, Huang B. Numerical investigation of the flow evolution of an oscillating foil with the different reduced frequency. E&ES 2018;163(1):012017.

[3] Yu M, Hu H, Wang Z. A numerical study of vortex-dominated flow around an oscillating airfoil with high-order spectral difference method. In: 48th AIAA Aerospace Sciences Meeting Including the New Horizons Forum and Aerospace Exposition; 2010. p. 726.

[4] Kurtulus DF. Unsteady aerodynamics of a pitching NACA 0012 airfoil at low Reynolds number. International Journal of Micro Air Vehicles 2019;11:1756829319890609.

[5] Pechloff DIA. Numerical simulation of a pitching NACA 0012 airfoil. In: 22nd International Congress of Aeronautical Sciences. Harrogate, UK: ICAS, vol. 773; 2000. p. 1–13.

[6] Karbasian HR, Kim KC. Numerical investigations on flow structure and behavior of vortices in the dynamic stall of an oscillating pitching hydrofoil. Ocean Engineering 2016;127:200–211.

[7] Lee T, Gerontakos P. Investigation of flow over an oscillating airfoil. Journal of Fluid Mechanics 2004;512:313.

[8] Sharma DM, Poddar K. Investigations on quasi-steady characteristics for an airfoil oscillating at low reduced frequencies. International Journal of Aerospace Engineering 2010;2010.

[9] SU2foundation, Governing Equations in SU2;. https://su2code.github.io/docs_v7/Theory/#incompressible-navier-stokes.

[10] Chorin AJ. A numerical method for solving incompressible viscous flow problems. Journal of computational physics 1997;135(2):118–125.

[11] SU2foundation, Convective Schemes;. https://su2code.github.io/docs_v7/Convective-Schemes/.

[12] SU2foundation, github/SU2/TestCases/rans/naca0012/;. https://github.com/su2code/TestCases/tree/master/rans/naca0012.

[13] Palacios F, Alonso J, Duraisamy K, Colonno M, Hicken J, Aranake A, et al. Stanford university unstructured (su 2): an open-source integrated computational environment for multi-physics simulation and design. In: 51st AIAA aerospace sciences meeting including the new horizons forum and aerospace exposition; 2013. p. 27–28.